World Journal of Advanced Research and Reviews

eISSN: 2581-9615 CODEN (USA): WJARAI

Cross Ref DOI: 10.30574/wjarr

Journal homepage: https://wjarr.com/

(Research Article)

Check for updates

Georeferenced diagnosis of drainage structures in the city of Bouaflé using geospatial techniques and machine learning

Houebagnon Saint-Jean Patrick Coulibaly [1, *], Rock Armand Bouadou [2], Jean Claude Konin [3], Talnan Jean Honoré C [2] and Théophile Gnagne [2]

[1] *Department of Space Sciences and Geomatics, Félix Houphouët-Boigny University, Côte d'Ivoire.*
[2] *Faculty of Environmental Science and Management, Nangui Abrogoua University, Côte d'Ivoire.*
[3] *Faculty of Governance and Sustainable Development, Bondoukou University, Côte d'Ivoire.*

World Journal of Advanced Research and Reviews, 2025, 28(01), 557-570

Publication history: Received on 30 August 2025; revised on 03 October 2025; accepted on 06 October 2025

Article DOI: https://doi.org/10.30574/wjarr.2025.28.1.3446

Abstract

The traditional method of collecting and processing socio-economic, health and spatial identification data on urban water infrastructure is time-consuming and costly. To reduce costs, geospatial and machine learning (Random Forest) tools were used to establish the Bouaflé Drainage Master Plan. These tools made it possible to characterise and predict the condition of the hydraulic infrastructure. The thalwegs, extracted from altimetric data using connectivity algorithms, were cross-referenced with the road network to identify the collection points for individual structures. The theoretical points were verified in the field to draw up an inventory of the structures and assess their operating condition. Population density, elevations, and the distance of structures from roads and canals are among the variables included in the prediction model. Field data collection identified 102 crossing structures and 38 gutters over 13.69 km. The prediction model has a satisfactory accuracy of over 96%. The distance to the canals significantly impacts the accuracy of the model. Structures located far from the drainage network often fail due to poor hydraulic connectivity. The high impact of population density creates significant anthropogenic pressure on infrastructure. The algorithmic approach reduced the diagnostic phase from three months to one and a half, while also identifying problems and enabling solutions to be targeted more effectively. The trained model could be applied in similar contexts, even in the absence of data on the condition of structures.

Keywords: Random Forest; Hydraulic structure; Bouaflé; Geospatial

1. Introduction

Ensuring the proper functioning of urban drainage systems is a challenge in most cities in developing countries. As a result, the effects of climate change tend to exacerbate frequent flooding, as noted by (Andrés-Doménech et al., 2021 [2]). Urban areas are rapidly expanding beyond their traditional centres, creating sprawling peri-urban areas that often lack infrastructure and services (Angel et al., 2011 [1]). At the same time, urban drainage networks are not developing or modernizing at the same pace, and given the effects of climate change, the risk of flooding is increasing (Wu et al., 2018 [20]).

Urbanization has progressively increased the extent of impervious surfaces (Andrés-Doménech et al., 2021; Lapiński & Wiater 2018; Limthongsakul et al., 2017 [2], [10], [11]), such as roads, car parks and roofs, and a reduction in forest areas and other forms of open space that absorb rainwater. Changes in the water balance are mainly caused by an increase in impervious surfaces. This leads to significant changes in both the quality and quantity of runoff (Paul & Meyer 2001; Muller et al., 2020 [16], [14]).

* Corresponding author: Houebagnon Saint-Jean Patrick Coulibaly

Urbanisation in developing countries poses significant challenges in terms of planning and managing drainage networks (Mohammed et al., 2019 [12]). It is essential to understand the condition and performance of drainage infrastructure to ensure sustainable urban development, particularly in the context of rapid urbanisation and climate change (Francisco et al., 2022 [8]). Several factors need to be considered when assessing the effectiveness of an urban drainage system (Molzahn & Burke, 1986 [13]).

To plan repairs and enhance the performance of drainage structures, it is important to assess their condition and the factors contributing to their deterioration. In Côte d'Ivoire, these assessments are rarely conducted comprehensively and systematically at city level. Most studies focus on the design and installation of structures, with limited consideration given to monitoring and maintenance, both of which are essential for ensuring longevity. The traditional method of gathering, processing and identifying urban water infrastructure spatially is not only labour-intensive, but also costly. To reduce costs, the Bouaflé Drainage Master Plan was formulated using geospatial and machine learning tools (Random Forest). Bouaflé, a town located in central-western Côte d'Ivoire, faces significant challenges in stormwater management. Drainage systems, which are essential for flood prevention, are often inadequate. This may be due to congestion or poor design. In the context of increasing rainfall, it is crucial to assess these structures in order to prioritize the interventions of the relevant services. This involves conducting a spatial assessment of the hydraulic infrastructure of the city of Bouaflé using geospatial data and machine learning models, specifically the Random Forest method.

2. Materials and methods

2.1. Study area

Bouaflé is the capital of the Marahoué region. This crossroads town is an important part of the department of the same name in terms of its enormous economic, social and cultural potential. The town of Bouaflé is located approximately 294 kilometres from Abidjan (the economic capital of Côte d'Ivoire) and 59 kilometres from Yamoussoukro (the political capital of Côte d'Ivoire). It is situated between longitudes 5°48' and 5°42' west and latitudes 6°57' and 7°3' north (Figure 1). The urban area of Bouaflé covers an area of 45 km². Bouaflé is traversed by the Marahoué River. According to the National Institute of Statistics, Bouaflé has a population of 109,186. The urban area of Bouaflé consists of 19 neighbourhoods : Agbanou, Bellou, Biaka-boda, Bromacote, Centre-administratif, Datecoumana, Dehita, Dioulabougou, Dioulabougou-Extension, Hermankono, Koblata, Koko, Lopoifla, Marahoue, Millionnaire, N'gatakro, Port-Bouet, Residentiel Est, Solibra.

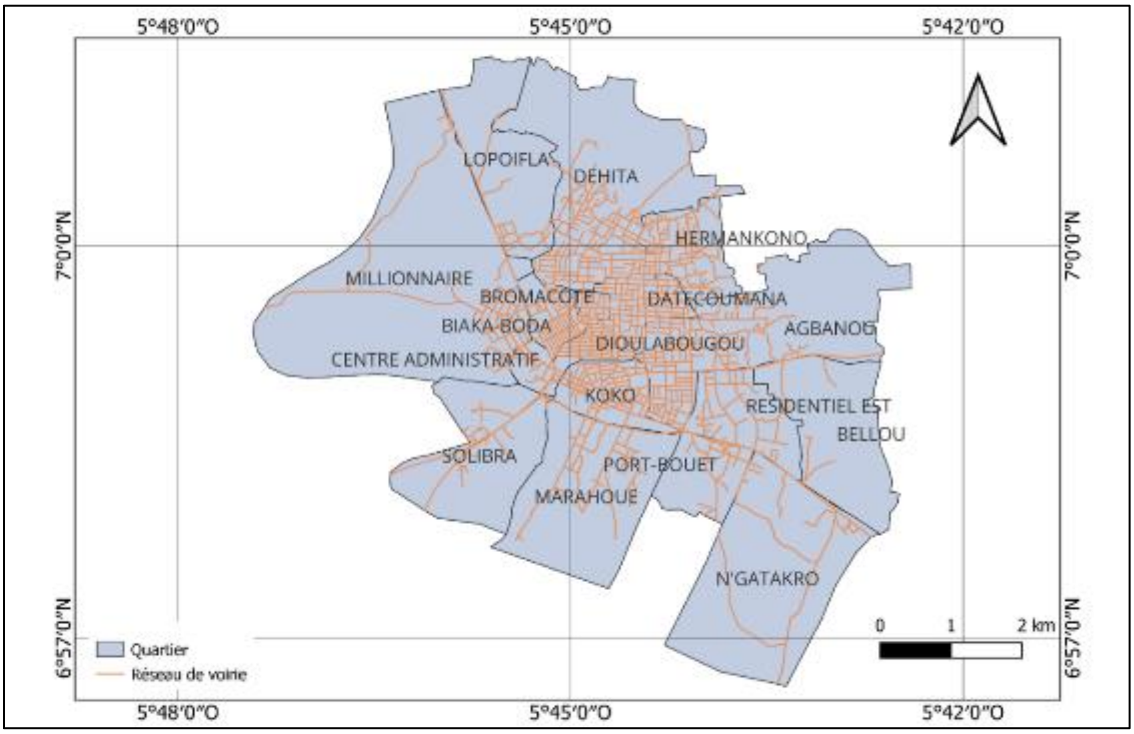

Figure 1 Neighbourhood in the town of Bouaflé

The town of Bouaflé is characterized by generally flat terrain. The municipality is located in a basin along the banks of the Marahoué River. The altitude of the urban area of Bouaflé varie between 156 and 257 metres above sea level. According to the soil classification system developed by FAO et al (1999) [6], the study area is dominated by ferric Acrisols and ferric Cambisols (Af). Acrisols are highly acidic clay soils with low cation exchange capacity and low base saturation. In the town of Bouaflé, ferric cambisols (Bf) are also found, which are thick soils with a silty-sandy texture. These soils are well suited to agriculture and are ideal for cocoa cultivation. Average annual rainfall is around 1,200 millimetres. The town of Bouaflé is characterised by four distinct rainy seasons: two dry seasons and two rainy seasons, a long dry season from November to March, a long rainy season from April to June, a short dry season from July to August, and a short rainy season from September to October. Average temperatures in Bouaflé range from 24.7°C (minimum) to 27.9°C (maximum) according to SODEXAM. The town is drained by the Marahoué River and some of its tributaries. The town has a dense hydrographic network. These natural waterways are characterised by the presence of two main rivers, the Frako and the Glopeny. The river system reflects the rainfall pattern.

2.2. Data and materials

2.2.1. Geospatial data

This type of data consists of:

- Road network (roads, tracks) represented as polylines, obtained from the CCT (Centre for Cartography and Remote Sensing);
- Open Street Map vector maps;
- Mosaic of satellite and aerial images, from Google Earth;
- Sentinel-2 images (level 2A, resolution 10–20 m), acquired from the Copernicus programme and used to calculate spectral indices;
- SRTM Digital Elevation Model (DEM) with 30 m resolution, available for download via the USGS Earth Explorer platform.

2.2.2. Population data

The high-resolution population data, comes from the WorldPop database for 2023 hosted by the University of Southampton. This database provides high-resolution annual estimates (from 100 m to 1 km depending on the product). They are derived from :

- National and regional population censuses;
- United Nations population projections (CIESIN (Centre for International Earth Science Information Network), (2018) [5];
- UNFPA (United Nations Population Fund);
- Auxiliary geospatial data (land use, road networks, infrastructure, altimetry, satellite imagery, OpenStreetMap, Microsoft Building Footprints, Microsoft Roads Dectior).

For this study, WorldPop population data with a resolution of 100 metres was used.

2.2.3. Data on drainage structures

A georeferenced inventory of drainage structures was conducted in 2023 in the urban area of Bouaflé using GPS during field surveys.

2.2.4. Data collection and processing tools

A series of software programs and tools were used to collect and process the data required for this study. These included:

- Qgis for geoprocessing and map production;
- Rstudio, for statistical analysis and model training;
- GPS for collecting geographical coordinates;
- Qfield for collecting data on hydraulic structures.

2.3. Methodology

The analyses were carried out using three main geospatial layers;

- Road network (roads, tracks, paths) represented as polylines ;
- Hydrographic network of thalwegs extracted from an SRTM Digital Elevation Model (DEM);
- Sentinel 2 satellite image.

2.3.1. *Extraction of potential sites for the placement of individual drainage structures*

It is carried out in two main stages: first, extracting the thalwegs and watercourses from the study area, and second, cross-referencing them with the road network data.

Extraction of thalwegs from the DEM

- *Pre-processing of the DEM*

The raw DEM often contains artificial depressions or 'sinks' that interrupt the flow network. These depressions must be filled in to ensure hydrological continuity (Crave, 1995 [4]), (Wang et Liu, 2006 [19]).

The operation known as sink filling consists of creating a modified DEM, Zf (x,y) such that: Zf (x,y) ≥ Zf (x,y), ∀ (x,y).

- *Extraction of the hydrographic network and delineation of Sub-Catchment Areas*

For the study, the D8 connectivity algorithm was applied to extract the drainage network. The direction 8 method was introduced by O'Callaghan et Mark (1984) [15].

Algorithm: Min [(Z (x, y) -z (xi, yi)]

Où xi= (x-1, x, x+1) ; yi= (y-1, y, y+1) ; Equation (1)

Z (x, y): Elevation of the central pixel.

z (xi, yi): Elevations of the 8 neighbours.

Identification of road–thaleweg crossing points

The aim is to identify road–thalweg intersection points to determine potential locations for hydraulic crossing structures (culverts, drains). To achieve this, a 10 m buffer zone was generated around the road network polylines. Intersections were then detected using the following equation: let X represent the buffered polygon of the road network and Y the thalweg network. The intersections are given by : $P = X \cap Y$.

Where P represents the probable crossing points, i.e., the potential locations for culverts or pipes.

2.3.2. *Collection of drainage structures (pipes, culverts, channels) Hydraulic interpretation and field validation*

The road–thalweg crossing points identified through topographical analysis are ideal locations for the installation of drainage structures. Intersections between roads and thalwegs represent zones where runoff from adjacent slopes intersects with the roadway. This intersection creates an increased risk of erosion or overflow. The relevance of these locations has been validated by field observations, revealing recurrent water stagnation during or after rainfall events. This comprehensive methodology, which merges hydraulic assessments with empirical field validation, reinforces the reliability of site selection for the implementation of suitable drainage solutions.

2.3.3. *Preparation of predictor variables*

The Sentinel-2 imagery underwent atmospheric correction and was subsequently cropped to focus on the study region. Both raster and vector data layers were reprojected to conform to the WGS 84 / UTM Zone 29N coordinate system. Population and elevation datasets were aligned with the resolution of the Sentinel-2 images (10 m) through bilinear resampling techniques. The integrity of the road and canal networks was confirmed through topological verification in QGIS 3.30.

Calculation of spectral indices

Two indices were calculated from Sentinel-2 bands :

- SAVI : Soil Adjusted Vegetation Index

SAVI is a vegetation index that corrects for the influence of bare soil on vegetation measurements, particularly useful in areas with sparse vegetation cover (urban areas) (Huete A. R. 1988 [9]). This index is used to quantify vegetation cover around hydraulic structures.

$$\mathrm{SAVI} = \frac{\mathrm{NIR-RED}}{\mathrm{NIR+RED+L}} \cdot (1 + \mathrm{L}) \qquad \text{Equation (2)}$$

Where NIR = B8, RED =B4 et L= 0.5 to limit the influence of the soil.

Values approaching 0 suggest minimal or absent vegetation, whereas values nearing 1 indicate robust and thriving vegetation.

- NDBI: Normalized Difference Built-up Index

The NDBI index was calculated to quantify the degree of urbanization around each hydraulic structure. It reflects the extent of soil sealing and its impact on the local hydrological regime Zha, Y., Gao, J., & Ni, S. (2003) [21].

$$\mathrm{NDBI} = \frac{\mathrm{SWIR-NIR}}{\mathrm{SWIR+NIR}} \cdot (1 + \mathrm{L}) \qquad \text{Equation (3)}$$

Avec SWIR = B11 et NIR =B8

Population density

Population data, disaggregated for this analysis, were sourced from WorldPop (Tatem, 2017 [18]). WorldPop employs spatial modeling techniques that leverage satellite imagery in conjunction with census information. For the purposes of this research, the WorldPop 2023 dataset was utilized, and population density values closest to each structure were extracted through spatial join. This metric acted as a proxy for assessing population pressure within the model proposed by Stevens et al. (2022) [17].

Elevation

Altitude data were retrieved from the SRTM Digital Elevation Model (DEM), which has a resolution of 30 meters, by conducting spot sampling at each structure's location (Farr et al., 2007 [7]).

Distances to roads and canals

The shortest Euclidean distances from each structure to the surrounding road and canal networks were computed using QGIS's Distance Matrix functionality.

Integration into the geospatial analysis database

All derived variables, including SAVI, NDBI, population density, elevation and distances to roads and canals, were integrated into the attribute table associated with drainage structures. This comprehensive database will serve as the foundation for subsequent statistical and predictive analyses.

2.3.4. Predictive modelling of hydraulic structure condition

Theoretical points identified through GIS and topographical analyses were verified in the field to create a comprehensive inventory of urban drainage structures. During these visits, the location of each structure was determined, and its operating condition was assessed according to standardised criteria (good or damaged). This phase allowed us to validate the theoretical data and collect detailed information on the existing infrastructure. A Random Forest machine learning model was created to forecast the operational status of drainage systems based on explanatory variables.

2.3.4.1. Target variable:

The observed condition of the structures, as determined by field data collection, was considered a dependent variable with two qualitative categories: 'good' and 'damaged'.

Explanatory variables

Several explanatory variables were included in the model to represent the condition of structures.

- Population density, which is an indicator of the pressure placed on infrastructure by human activity;
- Elevation, derived from the digital terrain model, was used to estimate the vulnerability of structures based on topography;
- Distance to roads and canals to quantify hydraulic connectivity and accessibility of structures;
- The SAVI spectral index indicates the presence of vegetation, which can signify obstruction, abnormal humidity or lack of maintenance;
- The NDBI spectral index, which measures urban pressure and impermeability (i.e. the level of stress and risk of damage to structures).

Thus, each structure is represented by a vector of predictors. The Random Forest (RF) algorithm (Breiman 2001 [3]) was applied to predict the condition of drainage structures based on environmental and socio-spatial explanatory variables.

Construction des arbres

Random Forest (RF) is based on the concept of decision trees, which are formed from the results of numerous independently generated trees. This strategy avoids overfitting, improves accuracy and offers greater robustness (Zhang et al., 2025 [22]). The condition of drainage structures (either 'good' or 'damaged') was predicted using the RF algorithm, which involves building a set of decision trees on bootstrap samples using a random subset of variables at each node. The final prediction for each structure is obtained by majority vote of the trees. The model's performance was evaluated using a confusion matrix and variable importance, which allowed the most influential factors affecting the condition of the structures to be identified. The condition of drainage structures (Y = Good or Damaged) was predicted using the RF algorithm, which is based on the aggregation of T decision trees built on bootstrap samples. For each tree t, a prediction $\widehat{f}_t(X)$ is produced based on the explanatory variables X = (X_1, ..., X_p).

$$\widehat{f}_t(X) = \sum_{m=1}^{M} c_m \ 1\{x \in R_m\} \qquad \text{Equation (4)}$$

Where $\boldsymbol{R_m}$ is the region corresponding to leaf M et m, c_m is the majority class in that leaf. The final prediction of the forest is obtained by a majority vote.

$$\hat{Y} = \text{mode}\{\widehat{f}_1(X), \widehat{f}_2(X), \dots, \widehat{f}_T(X)\} \qquad \text{Equation (5)}$$

The model's performance was evaluated using a confusion matrix and variable importance. This enabled the identification of the factors that have the greatest influence on the condition of structures.

Model evaluation

We evaluated the model's overall performance using the out-of-bag (OOB) error and the confusion matrix. This allowed us to estimate the model's accuracy, as well as its sensitivity and specificity. Thanks to Random Forest's internal cross-validation principle, these metrics provide a robust evaluation without the need for an external test set. Additionally, the importance of each variable was measured using Mean Decrease Accuracy (MDA), reflecting its contribution to the model's accuracy. MDA is based on the idea that if a variable is informative, permuting its values at random will significantly deteriorate predictive performance. Mathematically, the MDA for variable i is defined as follows:

$$MDA_{\text{i}} = (1/N) \times \sum[OOB_{\text{j}} - OOB_{\text{j, i}}{}^{\text{perm}}] pour\ j = 1 à N \qquad \text{Equation (6)}$$

- $MDA_{(i)}$: The importance of the variable i, according to the Mean Decrease in Accuracy.
- N: Number of observations
- OOB_j: Prediction error for observation j in the out-of-bag (OOB) sample.

- $OOB_{j,i}^{perm}$: Error obtained in observation j after permutation of variable i
- $\sum$: Sum of all observation samples.

3. Results and discussion

3.2. Watercourses and thalweg in the urban area of Bouaflé

Figure 2 illustrates the dense hydrographic network in the area. The Marahoué River and the two main tributaries, the Frako and the Glopeny, flow through the city of Bouaflé. This puts the population of Bouaflé at significant risk of flooding. Therefore, it is necessary to establish an effective drainage system in Bouaflé.

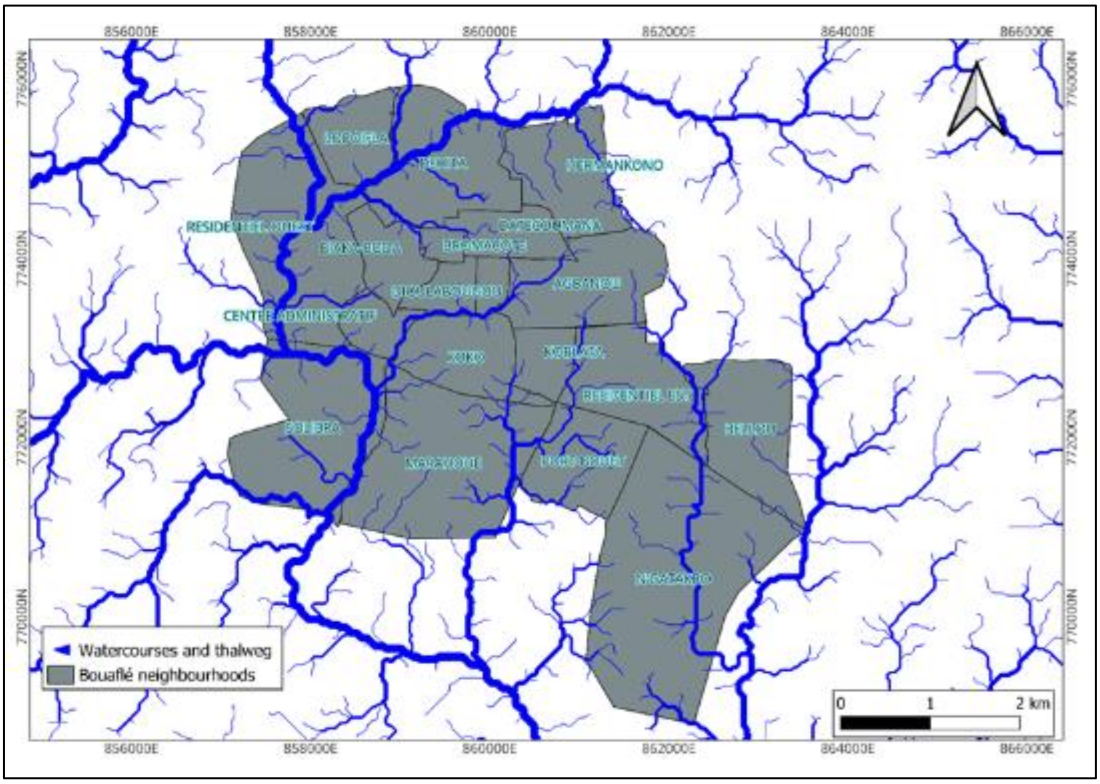

Figure 2 Watercourses and thalweg in the urban area of Bouaflé**.**

3.3. Potential sites for positioning individual drainage structures

Field data collection identified 312 potential drainage structures. These locations could accommodate culverts, drains or bridges. The high number of potential sites indicates the density of thalwegs in the urban area of Bouaflé (see Figure 3).

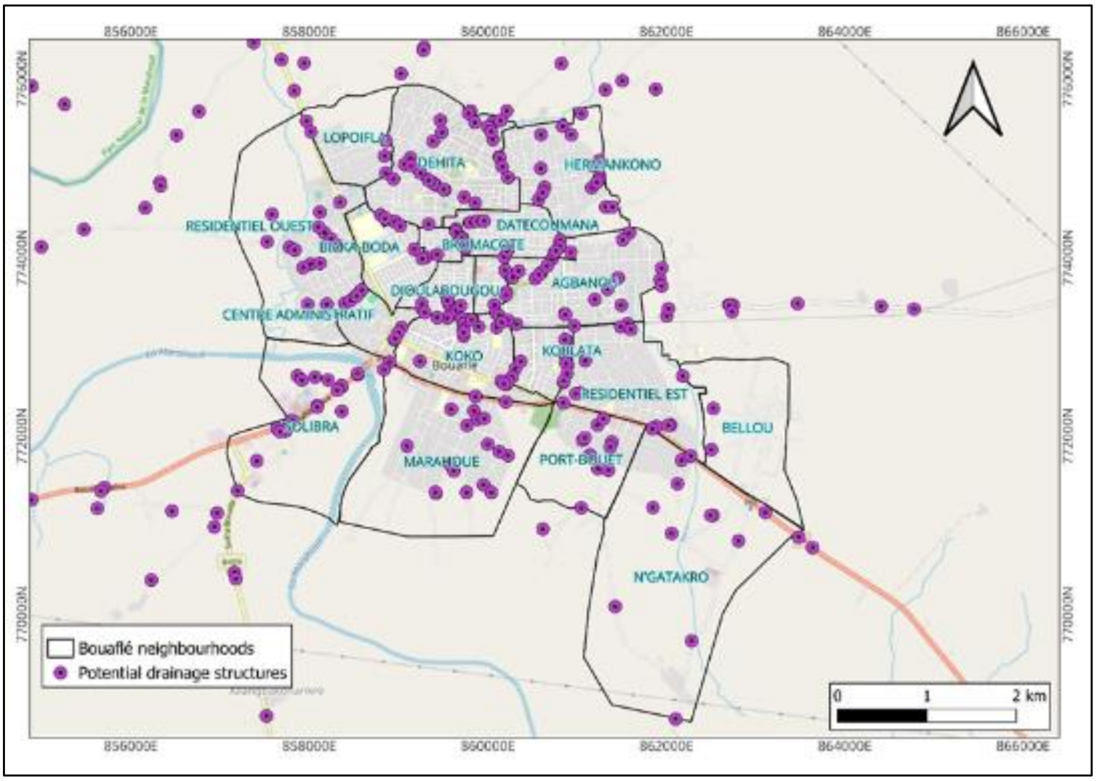

Figure 3 Potential drainage structures in the urban area of Bouaflé.

3.4. Identifying potential drainage structures in the field.

A systematic field survey (Figure 4) was carried out to identify existing unique drainage structures. This survey identified 102 crossing structures and 38 gutters along a 13.69 km stretch of land. The characteristics and geographical locations of these structures were also recorded.

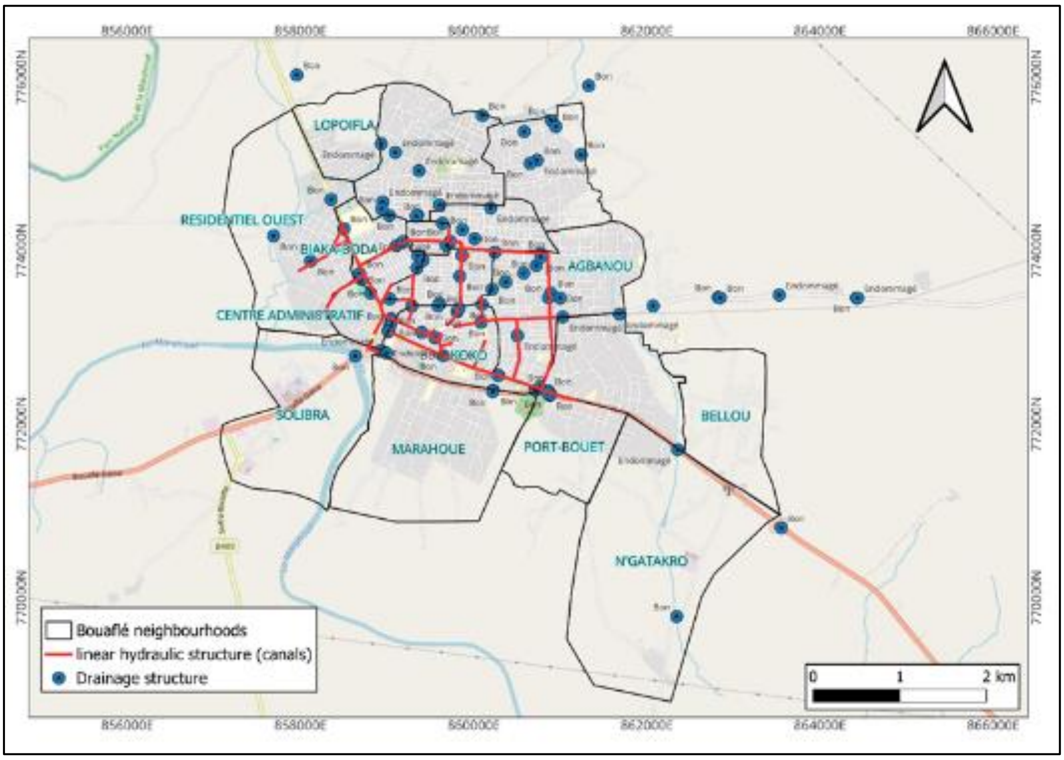

Figure 4 Drainage structure in the urban area of Bouaflé.

3.5. Results relating to explanatory variables.

3.5.1. Spectral indices

SAVI: Soil Adjusted Vegetation Index

Typical SAVI values for the urban area of Bouaflé are low. They range from -0.02 to 0.25 (see Figure 5). There is existing but sparse vegetation cover. This is a protective rather than a risk factor.

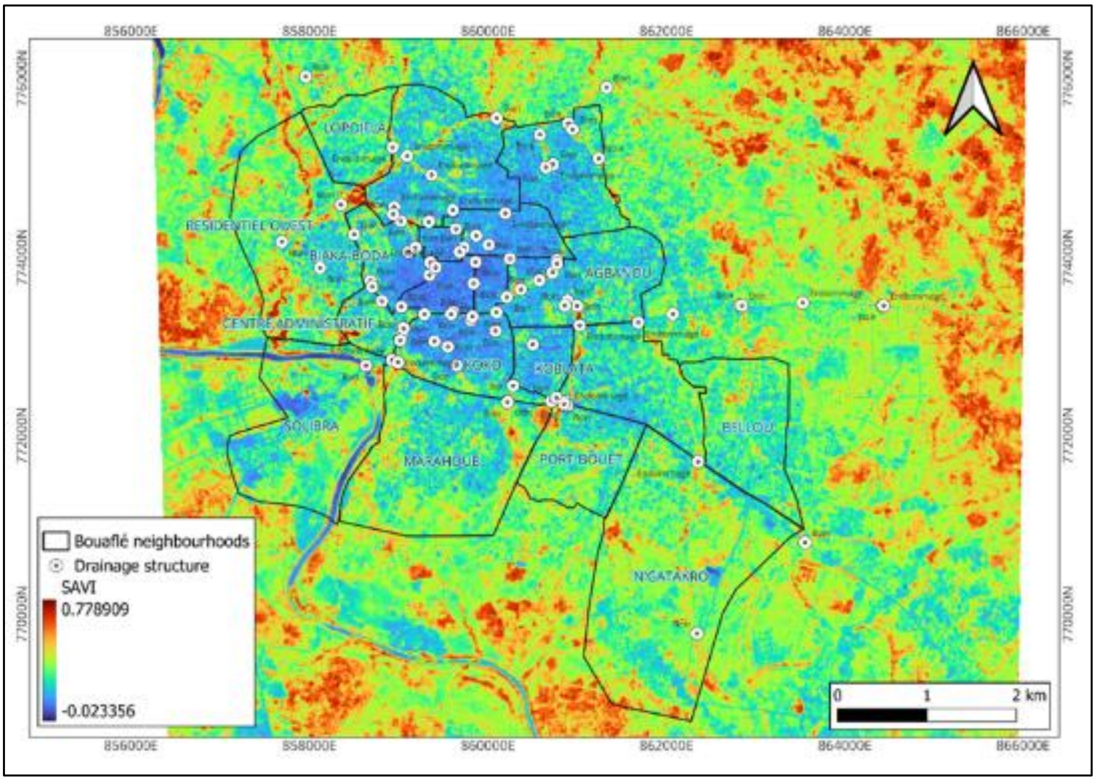

Figure 5 Soil Adjusted Vegetation Index of Bouaflé urban area

NDBI: Normalized Difference Built-up Index

The prominent position of the NDBI in our model highlights the significant effect that urbanisation has on the deterioration of hydraulic infrastructure. This highlights the importance of urban planning in the sustainable management of such structures. In Bouaflé, most structures are in areas with low permeability and NDBI values below 0.15 (see Figure 6).

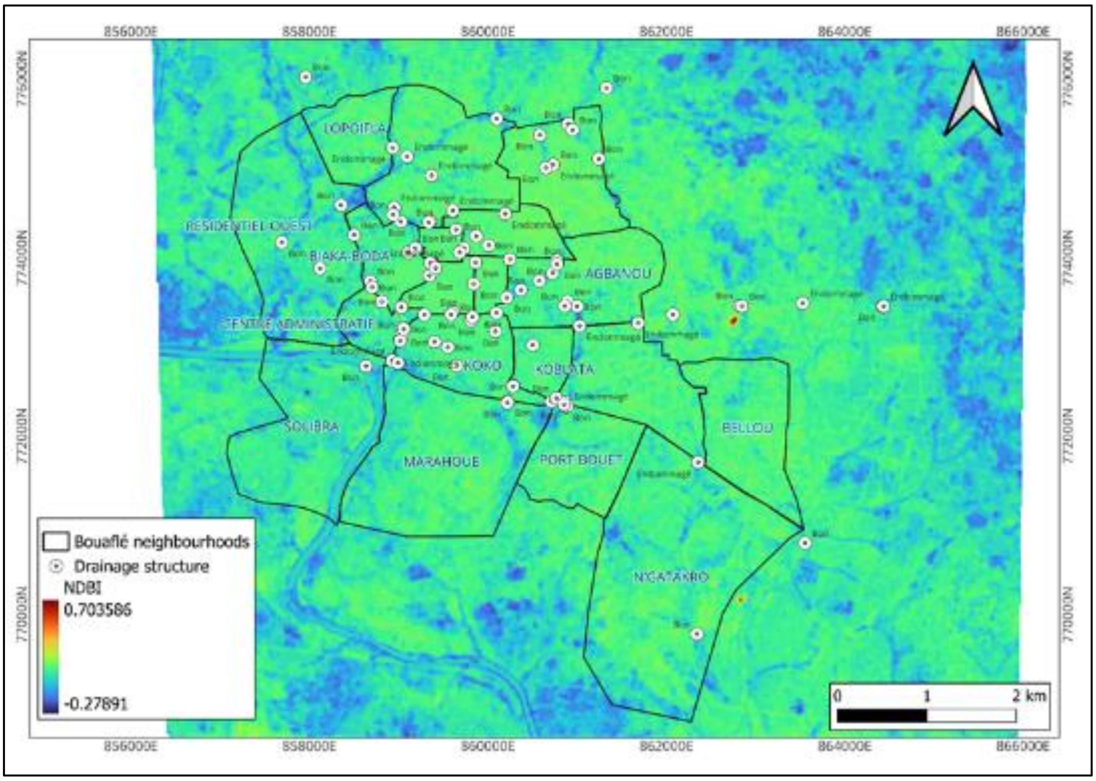

Figure 6 Normalised Difference Built-up Index of Bouaflé urban area

3.6. Predictive modelling using Random Forest

3.6.1. Performance of the binary classification model for quality control

The binary classification model, which was designed to distinguish between 'good' and 'damaged' works, performed well. It achieved an overall accuracy of 99.02%. No faulty structures were ignored (there were 0 false negatives), meaning that the system guaranteed that no 'damaged' structures were detected as 'good' (see Table 1).

Table 1 Prediction performance based on conditions

	Predicted: good	**Predicted: damaged**
Real : Good	72 (True Positive)	0 (False Negative)
Real : Damaged	1 (False Positive)	29 (True Negative)

- *Key performance metrics:*
  - Accuracy: 99.02%
  - Sensitivity (recall – 'good'): 100.00%
  - Specificity (Damaged'): 96.67%
  - Precision (Accuracy – 'Good') 98.63%
  - Negative predictive value (damaged): 100.00%
  - Kappa score: 0.976 (almost perfect agreement).

3.6.2. Analysis of the importance of variables for a classification model

Analysis of the importance of variables based on a Random Forest model reveals concordance between dist_canal and NDBI, which maintain their first and second positions respectively. Dist_canal emerges as the predominant factor, emphasising the significance of proximal hydraulic constraints. Structures near canals are exposed to accelerated bank erosion, hydraulic overloads during floods and sediment accumulation. The NDBI confirms that land artificialization has an impact on the deterioration of structures. Urbanization leads to an increase in runoff coefficients, an acceleration in peak flows and a change to natural hydrological regimes. However, there is a divergence between the MeanDecreaseGini and MeanDecreaseAccuracy rankings of elevation and population density values.

Elevation's high position in MeanDecreaseGini reflects its ability to create clear spatial distinctions. This variable acts as an indirect indicator of position within the catchment area, exposure to flow concentrations and the risk of waterlogging in low-lying areas. The relative decrease in population density in MeanDecreaseGini suggests a more diffuse effect linked to the complexity of anthropogenic pressures, variable obstruction phenomena and heterogeneous maintenance practices.

Finally, dist_route remains the least important variable in both metrics. This variable proves to be an uninformative, even harmful, predictor for this specific model. To simplify the model and improve its performance, dist_route could be excluded from future iterations without any loss of accuracy and potentially with an improvement in accuracy (see Figure 7).

Dist_canal : Distances to canals / Dist_roads : Distances to roads / Population density: densite_pop / SAVI: Soil Adjusted Vegetation Index / NDBI : Normalised Difference Built-up Index

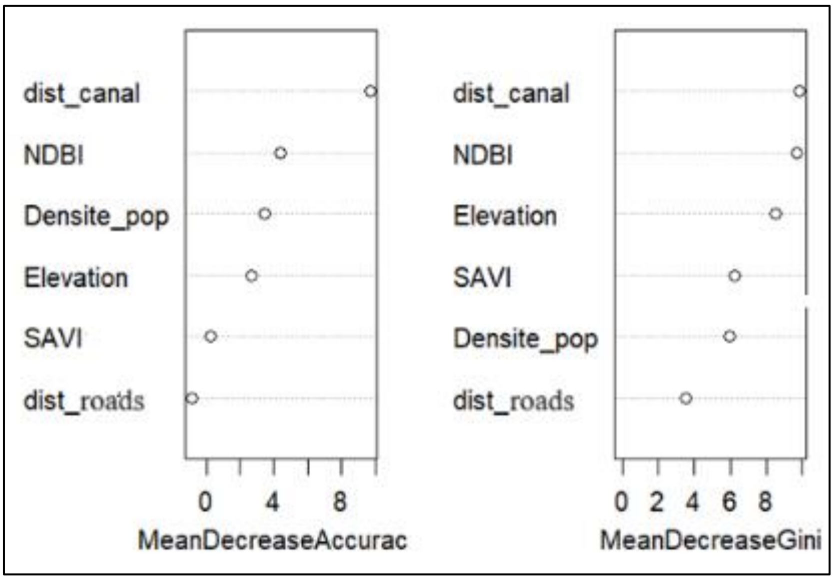

Figure 7 Ranking of variables by importance according to MeanDecreaseAccuracy and MeanDecreaseGini

3.6.3. Analysis of cartographic results

The predictive map generated by the Random Forest model (see Figure 8) distinguishes between three categories: structures in good condition; damaged structures; and areas with missing data.

The results show a high concentration of structures in good condition in the southern and south-western suburbs (Marahoué, N'gatakro and Port-Goué), while damaged structures are mainly found in densely populated central areas (the Administrative Centre, Koko, Residential West and Déhita). Peripheral areas not covered correspond to places where no data is available or where no structures have been surveyed. Recently urbanised areas, where structures are new or lightly used, generally have good working order. Conversely, central neighbourhoods characterised by high population density, significant impermeability and strong anthropogenic pressure account for most damaged structures.

The Random Forest model proved effective in distinguishing between structure conditions, achieving an accuracy of over 90% in the validation phases. Integrating explanatory variables derived from geospatial data (population density, NDBI and SAVI spectral indices, elevation and distance to roads and canals) enabled the main determinants of degradation to be captured. This demonstrates the ability of the Random Forest model to integrate multiple geospatial variables (population density, spectral indices, elevation and distance to roads and canals) to accurately predict the condition of structures (Figure 8).

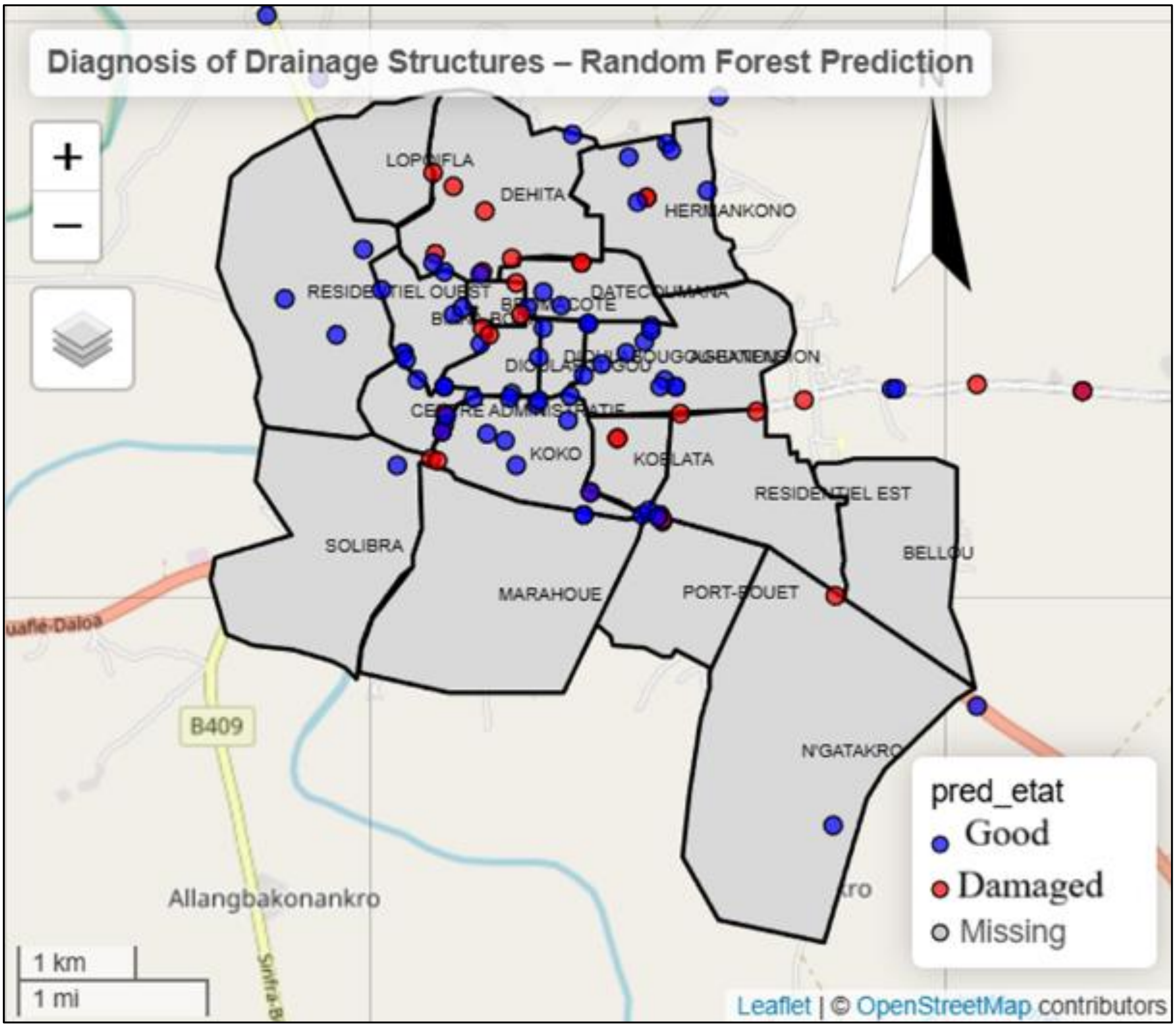

Figure 8 A predictive map for diagnosing drainage structures (culverts and pipes)

4. Conclusion

These results confirm the importance of using GIS and artificial intelligence in diagnosing urban infrastructure. Proactive planning enables the development of a differentiated strategy combining the rehabilitation of central areas with preventive maintenance in peripheral areas. Using geospatial data (NDVI, NDBI, population density and proximity to roads and canals), coupled with machine learning, provides a reproducible methodology that can be used in other cities facing similar issues. Mapping diagnostics facilitates the identification of critical points, which is essential in a context of rapid urbanisation and climate change where flooding risks are increasing. This approach could help to improve urban resilience to flooding in such contexts.

Compliance with ethical standards

Acknowledgments

This research was funded by Côte d'Ivoire's Ministry of Hydraulics.

Disclosure of conflict of interest

There is no conflict of interest to declare.

References

[1] Angel, S. et al. (2011). Making Room for a Planet of Cities. Lincoln Institute of Land Policy.

[2] Andrés-Doménech, I.; Anta, J.; Perales-Momparler, S.; Rodriguez-Hernandez, J. Sustainable Urban Drainage Systems in Spain: A Diagnosis. Sustainability 2021, 13, 2791. [Google Scholar] [CrossRef]

[3] Breiman, L. (2001). Random Forests. Machine Learning, 45(1), 5–32. https://doi.org/10.1023/A:1010933404324

[4] Crave, A. (1995). Quantification de l'organisation des réseaux hydrographiques. Thèse, Université de Rennes I, 209 p.

[5] Center for International Earth Science Information Network (CIESIN), Columbia University. (2018). Gridded Population of the World, Version 4 (GPWv4): Population Count, Revision 11. NASA Socioeconomic Data and Applications Center (SEDAC). https://doi.org/10.7927/H4JW8BX5

[6] FAO, ISRIC (Centre international de référence et d'information pédologique) et AISS (Association Internationale de la Science du Sol) (1999). Base de référence mondiale pour les ressources en sols. M-51. ISBN 92-5-304141-9. Rapport sur les ressources en sol du monde N°8, 496 p.

[7] Farr, T. G., Rosen, P. A., Caro, E., Crippen, R., Duren, R., Hensley, S., Kobrick, M., Paller, M., Rodriguez, E., Roth, L., Seal, D., Shaffer, S. (2007). The Shuttle Radar Topography Mission. Reviews of Geophysics, 45(2), RG2004. https://doi.org/10.1029/2005RG000183

[8] Francisco, T. H. S., Menezes, O. V. C., Guedes, A. L. A., Maquera, G., Neto, D. C. V., Longo, O. C., Chinelli, C. K., & Soares, C. A. P. (2023). The Main Challenges for Improving Urban Drainage Systems from the Perspective of Brazilian Professionals. Infrastructures, 8(1), 5. https://doi.org/10.3390/infrastructures8010005

[9] Huete, A. R. (1988). A soil-adjusted vegetation index (SAVI). Remote Sensing of Environment, 25(3), 295-309.

[10] Lapiński, D.; Wiater, J. Contamination content introduced with rainwater to the rivers after they have been cleaned in separators of petroleum compounds. Water, Wastewater and Energy in Smart Cities. E3S Web Conf. 2018, 30, 01019. [Google Scholar] [CrossRef]

[11] Limthongsakul, S.; Nitivattananon, V.; Arifwidodo, G. D. Localized flooding and autonomous adaptation in peri-urban Bangkok. Environ. Urban. 2017, 29, 51–68. [Google Scholar] [CrossRef]

[12] Mohammed, A., Iliyasu, A. M., Umar, G., Musa, D., Thomas, C. B., & Tukur, F. A. (2019). Assessment of the Effect of Inadequate Drainage Network on the Environment and Infrastructures. The International Journal of Science & Technoledge, 7(7). https://doi.org/10.24940/theijst/2019/v7/i7/ST1907-028

[13] Molzahn, R. E., & Burke, C. B. (1986). Assessment of drainage infrastructure for urban areas. Tunnelling and Underground Space Technology, 1(3–4), 387–389. https://doi.org/10.1016/0886-7798(86)90022-2

[14] Müller, A., Österlund, H., Marsalek, J., & Viklander, M. (2020). The pollution conveyed by urban runoff: A review of sources. Science of The Total Environment.

[15] O'Callaghan, J. F., & Mark, D. M. (1984). The extraction of drainage networks from digital elevation data. Computer Vision, Graphics, and Image Processing, 28(3), 323–344.

[16] Paul, M. J., & Meyer, J. L. (2001). Streams in the urban landscape: Urbanization and stream ecology. Annual Review of Ecology and Systematics, 32, 333–365.

[17] Stevens, F. R., Gaughan, A. E., Linard, C., & Tatem, A. J. (2022). Disaggregated population estimates for the contiguous United States in 2020 [Data set]. WorldPop. https://doi.org/10.5258/WORLDPOP/USA00PP20v1

[18] Tatem, A. J. (2017). WorldPop, open data for spatial demography. Scientific Data, 4(1), 170004. https://doi.org/10.1038/sdata.2017.4

[19] Wang, L. et Liu, H. (2006). An efficient method for identifying and filling surface depressions in Digital Elevation Models for Hydrologic analysis and modelling. International Journal of Geographical Information Science, 20, pp. 193–213.

[20] Wu, X., Wang, Z., Guo, S., Lai, C., & Chen, X. (2018). A simplified approach for flood modeling in urban environments. Hydrology Research, 49(6), 1804–1816. https://doi.org/10.2166/nh.2018.149

[21] Zha, Y., Gao, J., & Ni, S. (2003). Use of normalized difference built-up index in automatically mapping urban areas from TM imagery. International Journal of Remote Sensing, 24(3), 583–594.

[22] Zhang, D., Liu, J., Xiao, Y., Li, X., Chen, X., Zhong, P., & Ning, Z. (2025). Analysis of the Distribution Characteristics and Influencing Factors of Apparent Temperature in Chang–Zhu–Tan. Sustainability, 17, 7225. [Google Scholar] [CrossRef].